Journal of Electroceramics, 13, 177–182, 2004

The Photoresponse of Iron- and Carbon-Doped TiO_2 (Anatase) Photoelectrodes

CRISTINA S. ENACHE, JOOP SCHOONMAN & ROEL VAN DE KROL*

Laboratory for Inorganic Chemistry, Delft Institute for Sustainable Energy, Delft University of Technology, P.O. Box 5045, 2600 GA Delft, The Netherlands

Submitted February 13, 2003; Revised February 27, 2004; Accepted July 29, 2004

Abstract. Fe-doped and C-doped anatase TiO_2 films were made by spray pyrolysis. For Fe:TiO_2, a small sub-bandgap photoresponse is observed which is attributed to the presence of additional states located just above the valence band. Although no visible-light photoresponse is observed for carbon-doped TiO_2 due to the low carbon content, the photocurrent at $h\nu > E_g$ is significantly larger than for undoped TiO_2. At the same time, the donor density of oxidized C-doped TiO_2 is $>1.9 \times 10^{19}$ cm^{-3}, compared to 3.2×10^{17} cm^{-3} for undoped TiO_2. Assuming that only light absorbed in the depletion layer contributes to the photocurrent, the photoresponse of C-doped anatase (at 330 nm) is 16 times larger than that predicted for undoped TiO_2 under similar conditions. The strong enhancement of the absorption is most likely caused by a change in the electronic structure of the material due to the presence of carbon and/or related defects. Photoluminescence measurements suggest that the defects present in oxidized carbon-doped anatase resemble those present in undoped, reduced TiO_2.

Keywords: photocatalyst, titanium dioxide, anion dopants, photoluminescence, defects

Introduction

In 1972, Fujishima and Honda first demonstrated that water could be split into hydrogen and oxygen at a TiO_2 (rutile) photoanode under illumination with ultraviolet light [1]. Since then, many other photoelectrode materials have been investigated, but wide-bandgap transition metal oxides, in particular TiO_2, remain popular because of their high photochemical stability. A substantial part of the research on photocleavage of water by TiO_2 has been devoted to the use of transition metal dopants to improve the visible light photoresponse. These dopants introduce additional energy levels in the bandgap, so that sub-bandgap illumination can be used to excite electrons to the conduction band. While this works in principle, the efficiency of transition metal-doped photoelectrodes is still too low for practical use.

*To whom all correspondence should be addressed. E-mail: R.vandeKrol@tnw.tudelft.nl

The prospect of a future 'Hydrogen Economy' has renewed interest in the photocatalytic splitting of water. Recently, Asahi et al. showed that anion dopants can also be used to sensitize TiO_2 to visible light [2]. Promising results have already been obtained for anatase TiO_2 doped with nitrogen [3], and for rutile TiO_2 doped with carbon [4] or sulfur [5]. The p-orbitals of these anions show significant overlap with the valence band O-2p orbitals, which facilitates the transport of photo-generated charge carriers to the surface of the catalyst [2]. In contrast, transition metal dopants generally have strongly localized d-states deep in the bandgap. These often act as recombination centers and slow down hole transport.

In this work, the photoelectrochemical properties of iron- and carbon-doped anatase TiO_2 photoelectrodes are investigated. Compared to rutile TiO_2, the anatase phase is preferred because of its higher photocatalytic activity [6]. The results will be discussed in relation to the ionic defects present in the material, an important

aspect that is often ignored in studies on metal oxide photoelectrodes.

Experimental

Spray Pyrolysis (SP) was used to prepare undoped and Fe- and C-doped TiO_2 thin films. The precursor solution consisted of 2.4 ml TTiP (titanium-tetraisopropoxide, 99.999%) in 54 ml ethanol (>99.9%), with 3.6 ml acetyl-acetonate (99+%) added to prevent cracking of the films. Iron (Fe) was introduced as a dopant by adding iron nitrate in a ratio of Fe:Ti = 0.01. Carbon is incorporated as dopant by carrying out the deposition under a mixed CO_2/O_2 atmosphere. The substrate temperature was 350°C, and a 3s on, 60s off spraying-cycle was used. The film thickness was typically 100 ± 20 nm. F:SnO_2 on glass (Libbey Owens Ford) and fused silica (quartz, ESCO S1-UV) were used as substrates.

Photoelectrochemical measurements were performed in a three-electrode cell, with a platinum counter electrode and a saturated calomel reference electrode (SCE). An aqueous solution of 0.1 M KOH was used as an electrolyte. The potentiostat (Solartron 1286) used for current measurements was combined with a frequency response analyser (Solartron 1250) for impedance measurements. A 200 W tungsten halogen lamp in combination with a grating monochromator (Acton SPro 150) was used to irradiate the sample. High-pass filters (Schott) were used to remove the second order of the diffracted light. The light intensity was measured as a function of wavelength with a calibrated photodiode (PD 300-UV, Ophir).

Photoluminescence measurements were recorded with a home-built setup using a pulsed Nd:YVO_4 laser with a wavelength of 355 nm (Spectra Physics). The spectra were recorded in the back-scatter mode using a CCD camera cooled with liquid nitrogen (LN/CCD-1100PB, Princeton Instruments) and a grating monochromator (Spex 340E). Stray laser light was removed with two Supernotch filters (Kaiser Optical Systems). Corrections for the sensitivity of the CCD camera, monochromator, filters, and conversion from $I/d\lambda$ to E/dE (with a factor of λ^2) were applied. For low-temperature measurements a closed-cycle helium cryostat (APD Cryogenics CSW 204SL-6.5K) was used.

Results and Discussion

All deposited films are optically transparent, uniform, smooth, crack-free, and well adherent to the substrate. X-ray diffraction and Raman spectroscopy (not shown) reveal that as-deposited films are crystalline with clear anatase peaks. A post-deposition anneal at 450°C in air further improves the crystallinity of the films. Subsequent reduction of the Fe-doped films in an Ar:H_2 (10:1) mixture results in an anatase-to-rutile phase transformation, which has also been observed by Bally et al. [7]. No transformation to rutile is observed during a thermal anneal under oxidizing conditions. Furthermore, no traces of rutile or any other phases are observed after oxidation or reduction of undoped or C-doped anatase TiO_2 films.

To investigate the influence of Fe and C dopants on the optical properties of TiO_2, photocurrent spectra are recorded. The incident photon-to-current conversion efficiencies (IPCE) are shown in Fig. 1. The insert reveals an indirect bandgap of 3.26 ± 0.05 eV for undoped anatase TiO_2, in excellent agreement with previously reported values [8, 9]. For Fe-doped TiO_2, a small photocurrent is observed just below the bandgap. Bally et al. [7] observed a similar effect and attributed it to the presence of rutile, which has a smaller bandgap than anatase ($E_{g,rutile} = 3.05$ eV [10]). In our case, however, x-ray diffraction and Raman spectroscopy reveal no trace of rutile in the oxidized Fe:TiO_2 samples. A

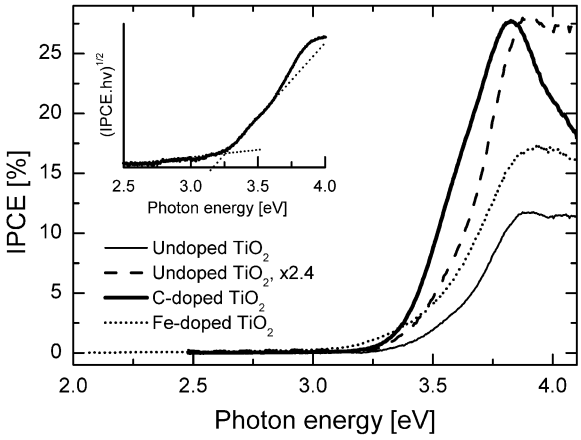

Fig. 1. Photocurrent action spectra of undoped, Fe-doped, and C-doped anatase TiO_2, recorded at a potential of 0 V vs. SCE. The insert shows the photocurrent spectra of undoped TiO_2, plotted as $(\text{IPCE}\times h\nu)^{1/2}$ vs. $h\nu$ to determine the bandgap of the TiO_2.

more likely explanation is that the Fe^{3+} dopants introduce sub-bandgap energy levels in anatase, located just above the valence band, from which electrons can be excited. A similar explanation has been offered for the small sub-bandgap photocurrents observed in Fe-doped rutile [11, 12].

In the case of C-doped anatase TiO_2 films, no photocurrent is observed in the visible part of the spectrum. Khan et al. observed significant optical absorption at $h\nu > 2.32$ eV for rutile TiO_2 heavily doped with carbon [4]. They also observed larger photocurrents than for undoped TiO_2 under white light illumination. Although one cannot directly compare optical absorption spectra to photocurrent action spectra (not all absorbed photons will result in an external current), it is obvious that the optical absorption of the present carbon-doped anatase is markedly different from that of carbon-doped rutile TiO_2. A further observation from Fig. 1 is that the band-to-band absorption ($h\nu > 3.2$ eV) of C-doped anatase is ~2.4 times stronger than that of undoped anatase. In a recent publication, Sakthivel et al. [13] also observed an enhanced UV photoresponse without any visible-light photoresponse for anatase TiO_2 containing 0.03% carbon. Since larger concentrations of carbon (e.g. 0.42%) do lead to a visible-light photoresponse [13], we conclude that the carbon content in our films is (too) low.

The film thickness of C:TiO_2 is approximately equal to that of undoped TiO_2, so this cannot explain the large increase in the UV photocurrent. However, if the minority carrier diffusion length is much smaller than the film thickness, as is generally the case in polycrystalline oxide semiconductors, the relevant parameter is not the film thickness but the depletion layer width, since only the photons that are absorbed in the depletion layer will contribute to the photocurrent. To determine the width of the depletion layer, capacitance measurements are carried out. The impedance spectrum shown in Fig. 2 (insert) reveals that the response of the system is purely capacitive between 1 and 50 kHz, and it is assumed that the overall response is dominated by the space charge capacitance. This allows us to determine the donor density and the space charge width from Mott-Schottky measurements [14]. The Mott-Schottky curves for undoped and carbon-doped anatase TiO_2, both oxidized in air, are shown in Fig. 2. The donor density, N_D, can be calculated from the slope of the curve according to:

$$\frac{1}{C^2} = \frac{2}{eN_D\varepsilon_0\varepsilon_r A^2}\left(\phi - \phi_{fb} - \frac{kT}{e}\right) \qquad (1)$$

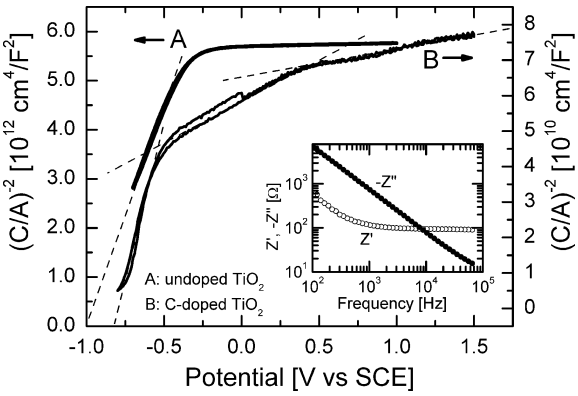

Fig. 2. Mott-Schottky plots of undoped and carbon-doped anatase TiO_2 (both oxidized at 450°C in air), recorded with frequencies of 10 and 2 kHz, respectively. The perturbation amplitude is 10 mV, the scan rate is 10 mV/s. The insert shows an impedance spectrum for undoped TiO_2 at 0 V vs. SCE, indicating the frequency range in which reliable Mott-Schottky data can be measured. The real part of the impedance at low frequencies represents the combined resistance of the leads, electrolyte, contacts, and TiO_2 bulk resistance (≈95 Ω).

Here, C is the capacitance, ϕ is the applied potential, ϕ_{fb} is the flat band potential, A is the surface area (=2.83 × 10^{-5} m^{-2}), ε_r is the relative dielectric constant (=55 [14]), and all other symbols have their usual meaning.

The flatband potential for undoped TiO_2 is −1.06 V vs. SCE, in good agreement with previous reports [14, 15]. For the C-doped film, ϕ_{fb} is shifted to a ~0.2 V more positive value, −0.83 V vs. SCE. The origin of this shift is not clear and calls for further investigation.

For as-deposited undoped TiO_2 a donor density of 1.5 × 10^{19} cm^{-3} is found. This value decreases to 3.2 × 10^{17} cm^{-3} after oxidation for 6 hours at 450°C in air (curve A). After an additional 12 hours at 450°C, the donor density decreases by another order of magnitude. These values are about as low as can be achieved for this oxide and demonstrates the high film quality that can be obtained with spray pyrolysis. The horizontal part of the curve at $\phi > -0.2$ V vs. SCE indicates that the film is fully depleted, as described in detail elsewhere [14]. For the carbon-doped TiO_2 (curve B), three distinct slopes are observed, corresponding to donor densities of 1.9 × 10^{19} cm^{-3}, 1.0 × 10^{20} cm^{-3}, and 2.8 × 10^{20} cm^{-3} (from left to right). These values are more than two orders of magnitude higher than for undoped TiO_2, despite the fact that both films have been oxidized at 450°C in air. The non-uniform

donor density indicates segregation of shallow donors or compensating acceptors away from or towards the surface, respectively. Before the post-deposition thermal anneal, the carbon-doped films show only a single slope, corresponding to a donor density of $\sim 10^{18}$ cm^{-3}. Hence, the post-deposition thermal anneal results in a segregation of dopants and a large increase in the density of shallow donors close to the surface. The origin of the shallow donors in anatase TiO_2 is still under debate, both oxygen vacancies and titanium interstitial have been proposed [16]. While the high donor density in carbon-doped anatase TiO_2 can most likely be attributed to one of these native defects, the possibility that carbon itself acts as a shallow donor cannot be entirely dismissed.

The high donor density implies a small depletion layer width, w, which can be calculated with:

$$w = \sqrt{\frac{2\varepsilon_0\varepsilon_r}{eN_D}\left(\phi - \phi_{fb} - \frac{kT}{e}\right)} \qquad (2)$$

At 0 V vs. SCE, the potential at which the photocurrent spectra in Fig. 1 are recorded, the depletion layer widths for undoped and C-doped TiO_2 are $\sim$115 nm (i.e., full depletion) and $\sim$12 nm, respectively. The fraction of the incident light absorbed in the depletion layer, f, can be calculated using Beer's law:

$$f(\alpha, w) = \frac{\int_0^w I_0 e^{-\alpha z}\, dz}{\int_0^\infty I_0 e^{-\alpha z'} dz'} = (1 - e^{-\alpha w}) \qquad (3)$$

Here, α is the absorption coefficient and I_0 is the light intensity at $z = 0$. Here, we assume that: i) only the light absorbed in the space charge (SC) region contributes to the photocurrent, and ii) all the light absorbed in the space charge region contributes to the photocurrent. With $\alpha \approx 9 \times 10^6$ m^{-1} at 330 nm for anatase TiO_2 [17], $f(\alpha,w)$ is $\sim$10% for the C-doped TiO_2, and $\sim$66% for undoped film. Therefore, the photocurrent of C-doped TiO_2 at 330 nm is expected to be $\sim$6.6 times smaller than that of undoped TiO_2. This factor is based solely on the values of w and α, assuming as we mention above that the photocurrent originates entirely from the photogenerated electron-hole pairs in the depletion layer.

To investigate why the measured photocurrents for carbon-doped anatase TiO_2 are $\sim 2.4 \times 6.6 = 16$ times higher (at 330 nm) than expected, two materials' parameters need to be considered. The first parameter is the dielectric constant of the material, which was assumed to be the same as that for undoped TiO_2. If one or more of the defects introduced by the carbon dopant results in a large increase in the dielectric constant, as is observed for anatase TiO_2 doped with Li [18] or H [19], the actual donor density is much smaller, and the depletion layer width is much larger than the values calculated above. While this effect may indeed occur, a larger value of w for the C:TiO_2 films does not explain a 2.4 times higher value for the measured photocurrent, since Fig. 1 shows that the undoped TiO_2 is fully depleted at 0 V vs. SCE. Further work is in progress to determine the actual value of the dielectric constant of C-doped TiO_2. For this, thinner films with a well known thickness are being used, following our previously reported approach [14].

The second parameter is the optical absorption coefficient of C-doped TiO_2. Asahi et al. calculated the density of states before and after substitutional doping of carbon on the oxygen anion sites in anatase TiO_2 [2]. Their calculations suggest the presence of additional states in the bandgap at $\sim$1 eV above the valence band, which is consistent with the visible-light photoresponse observed by others [4, 13]. However, no additional states were found that could explain the enhanced photocurrents at energies $>$3.2 eV. Therefore, it seems more likely that the enhanced photocurrent is related to changes in the electronic structure caused by other defects that are simultaneously introduced with carbon in order to satisfy the conservation of mass, charge, and lattice sites. Alternatively, carbon itself may reside on other sites than the oxygen anion sites, since it can have many different oxidation states and corresponding ionic radii.

To reveal the nature of the defects involved in undoped and doped anatase TiO_2, low-temperature photoluminescence (PL) measurements have been carried out. The results are shown in Fig. 3 for undoped and for carbon-doped anatase TiO_2. For undoped TiO_2, three peaks are observed. The peak at $\sim$2.4 eV is attributed to self-trapped excitons (STEs) [8, 20, 21]. Oxidation (A) or reduction (B) treatments do not significantly affect this peak, confirming its intrinsic character. The peak at $\sim$2 eV increases in intensity after reduction, and may be related to oxygen vacancies, titanium interstitials, or excitons bound to one of these defects. The broadening of this peak indicates an increase in the amount of disorder due to the increase in the number of defects upon reduction. The peak at $\sim$1.6 eV is significantly

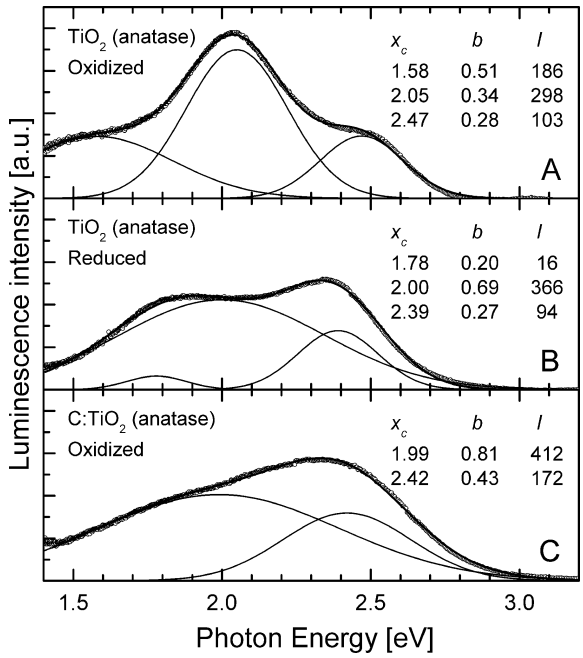

Fig. 3. Photoluminescence spectra of undoped and carbon-doped anatase TiO_2, measured at 10 K. Oxidation took place at 450°C in air, reduction at 450°C in an Ar/H_2 (10:1) mixture. The excitation wavelength is 355 nm (3.49 eV). The open circles are the measured data and the solid lines represent a fit of the data with Gaussian-shaped curves. The position (x_c), width (b), and integrated intensity (I) of the individual peaks are indicated.

shifted and virtually disappears after reduction. Hence, it is reasonable to assume that this peak is also related to the presence of ionic point defects, or to excitons bound to these defects. Since titanium vacancies are the only defects in undoped TiO_2 whose concentration increases with increasing oxygen partial pressure [22], we tentatively attribute the 1.6 eV peak to the presence of titanium vacancies.

The PL of oxidized carbon-doped anatase TiO_2 only shows the two peaks at 1.99 eV and 2.42 eV, indicating the presence of oxygen vacancies (and/or titanium interstitials) and STEs, respectively. The integrated intensities and widths of these peaks are significantly larger than those of reduced undoped TiO_2, indicating a large number of defects and substantial disorder. It should be noted that this disorder is not related to a decrease in the crystallinity, since XRD analysis shows well-defined anatase diffraction peaks for the carbon-doped samples. The similarities in the PL spectra of reduced undoped TiO_2 and oxidized carbon-doped TiO_2 suggest that the same types of defects are present. This provides an important clue for further work aimed to unravel the defect chemistry of carbon-doped anatase TiO_2.

Conclusions

The small, sub-bandgap photocurrent observed for Fe-doped anatase TiO_2 can be explained by Fe^{3+} dopants introducing additional energy levels in the bandgap, just above the valence band. The photoelectrochemical properties of carbon-doped anatase TiO_2 have been investigated for the first time. Little or no photocurrent is observed in the visible part of the spectrum, which is attributed to a (too) low carbon content. However, the photocurrent due to band-to-band excitation is significantly higher than that of undoped TiO_2, despite the high donor density and correspondingly small depletion layer in oxidized, C-doped anatase TiO_2. The origin of the enhanced photocurrent is most likely a change in the electronic structure of the material due to the incorporation of carbon and/or related defects. Although the exact nature and concentration of these defects is not known, photoluminescence measurements suggest that defects in oxidized carbon-doped anatase closely resemble those present in undoped, reduced TiO_2. Further work is aimed to determine the dielectric constant of C-doped anatase and to measure and control the concentration of carbon. Detailed knowledge of these parameters is required for a better understanding of the optical properties and defect chemistry of carbon-doped anatase TiO_2.

Acknowledgments

The authors would like to thank Dr. H. Donker for valuable discussions and kind assistance with the photoluminescence experiments. Financial support for this work is provided by the Delft Institute for Sustainable Energy, under the Sustainable Hydrogen program.

References

1. A. Fujishima and K. Honda, *Nature*, **238**, 37 (1972).
2. R. Asahi, T. Morikawa, T. Ohwaki, K. Aoki, and Y. Taga, *Science*, **293**, 269 (2001).
3. T. Morikawa, R. Asahi, T. Ohwaki, K. Aoki, and Y. Taga, *Jap. J. Appl. Phys.*, **40**(2), L561 (2001).

4. S.U.M. Khan, M. Al Shahry, and W.B. Ingler, *Science*, **297**, 2243 (2002).
5. T. Umebayashi, T. Yamaki, H. Itoh, and K. Asai, *Appl. Phys. Lett.*, **81**, 454 (2002).
6. A.L. Linsebigler, G. Lu, and J.T. Yates, *Chem. Rev.*, **95**, 735 (1995).
7. A.R. Bally, E.N. Korobeinikova, P.E. Schmid, F. Levy, and F. Bussy, *J. Phys. D*, **31**, 1149 (1998).
8. H. Tang, K. Prasad, R. Sanjinès, P.E. Schmid, and F. Lévy, *J. Appl. Phys.*, **75**, 2042 (1994).
9. H. Minoura, M. Nasu, and Y. Takahashi, *Ber. Bunsenges. Phys. Chem.*, **89**, 1064 (1985).
10. H. Tang, F. Levy, H. Berger, and P.E. Schmid, *Phys. Rev. B*, **52**, 7771 (1995).
11. H.P. Maruska and A.K. Ghosh, *Solar Energy Mater.*, **1**, 237 (1979).
12. K. Mizushima, M. Tanaka, A. Asai, S. Iida, and J.B. Goodenough, *J. Phys. Chem. Solids*, **40**, 1129 (1979).
13. S. Sakthivel and H. Kisch, *Angew. Chem. Int. Ed.*, **42**, 4908 (2003).
14. R. Van de Krol, A. Goossens, and J. Schoonman, *J. Electrochem. Soc.*, **144**, 1723 (1997).
15. F. Möllers, H.J. Tolle, and R. Memming, *J. Electrochem. Soc.*, **121**, 1160 (1974).
16. P. Knauth and H.L. Tuller, *J. Appl. Phys.*, **85**, 897 (1999).
17. H. Takikawa, T. Matsui, T. Sakakibara, A. Bendavid, and P. Martin, *Thin Solid Films*, **348**, 145 (1999).
18. R. Van de Krol, A. Goossens, and J. Schoonman, *J. Phys. Chem. B*, **103**, 7151 (1999).
19. M.F. Weber, L.C. Schumacher, and M.J. Dignam, *J. Electrochem. Soc.*, **129**, 2022 (1982).
20. N. Hosaka, T. Sekiya, and S. Kurita, *J. Lumin.*, **72**(4), 874 (1997).
21. M. Watanabe, S. Sasaki, and T. Hayashi, *J. Lumin.*, **87**(9), 1234 (2000).
22. D.M. Smyth, *The Defect Chemistry of Metal Oxides* (Oxford University Press, New York, 2000).